Fluoride Inhibition of Yeast Enolase. 1. Formation of the Ligand Complexes†

Peter J. Maurer and Thomas Nowak*,‡

ABSTRACT: The binding of fluoride ion (F^-) and inorganic phosphate (P_i) to the yeast enolase–Mn complex was investigated by UV difference and proton relaxation rate (PRR) techniques. The F^- and the P_i ligands induce characteristic UV difference spectra of the E–Mn complex which were used to quantitate the binding of these ligands. The studies were performed in the presence of excess Mn^{2+} ($[Mn^{2+}]/[E]_t$ = 8.0). The K_d value for F^- was 0.6 ± 0.2 M, and for P_i the K_d was 0.3 ± 0.1 mM. The quaternary, E–Mn–F–P_i, complex also showed a UV difference spectrum. The K_d value for F^- from the quaternary complex was <10 mM, and the K_d for P_i from the quaternary complex was 0.5 ± 0.2 μM, demonstrating a strong positive cooperativity in ligand binding. In the PRR studies, lower ratios of Mn^{2+} to enzyme, which had some effect on both P_i binding to enolase–Mn and on F^- binding to enolase–Mn–P_i, were used. The binary enolase–Mn complex has an enhancement of 13–15. Titration of the binary complex with F^- gave a ternary enhancement of 7 and a K_d value of 0.6 ± 0.1 M with either 0.7 or 3.0 Mn^{2+} per enolase dimer. Titration of the binary complex with P_i gave a ternary enhancement of 10 with a K_d of 1.2 ± 0.2 mM and 0.6 ± 0.1 mM with 0.64 and 2.5 Mn^{2+} per enolase dimer, respectively. Titration of the ternary complexes to form the quaternary enolase–Mn–P_i–F complex gave a final enhancement of 0.7. The K_d for P_i from the quaternary complex was 19 ± 2 μM and 1 μM with 0.65 and 2.8 Mn^{2+} per enolase dimer, respectively. The K_d for F^- was 2.4 ± 0.4 mM with 0.64 Mn^{2+} per enolase dimer. At 3.0 Mn^{2+} per enolase, a single K_d value is insufficient to fit the F^- binding data. The binding data were fit assuming two equivalent binding sites showing positive cooperativity for F^- with K_{d_1} = 7.2 ± 1.2 mM and K_{d_2} = 1.0 ± 0.4 mM. The binding data indicate a random addition of F^- and P_i to the enzyme–metal complex to produce the inactive enolase species. A temperature dependence of the PRR data for each complex was performed. The data indicate that F^- displaces a water molecule from the first coordination sphere of bound Mn^{2+}. The P_i appears to slow the exchange rate of a proton of bound water, perhaps by hydrogen bonding. The quaternary complex has no rapidly exchanging protons in the primary coordination sphere of the bound Mn^{2+}. The cation in the quaternary complex is highly shielded from the solvent environment, and relaxation of the water protons may reflect either an outer sphere effect or the effects of slow exchange.

Enolase [phosphoenolpyruvate hydratase (EC 4.2.1.11)] is a glycolytic enzyme which catalyzes the reversible dehydration of 2-PGA[1] to yield P-enolpyruvate. This enzyme has an absolute requirement for a divalent cation for enzymatic activity which can be fulfilled by a variety of metal ions (Wold & Ballou, 1957). Enolase was shown to be the target enzyme for the inhibition of glycolysis by fluoride ion (Warburg & Christian, 1941–1942). Warburg & Christian demonstrated that the inhibition of enolase by F^- was quite weak. However, in the presence of P_i (an intracellular physiological buffer) the inhibition of the Mg^{2+} activated enzyme was extremely potent. A linear relationship between the inhibition index, i (the fraction of inhibited enzyme/fraction of uninhibited enzyme), and $[M^{2+}][P_i][F^-]^2$ was described. The loss of an active enzyme–metal complex was postulated due to the binding of 1 equiv of P_i and 2 equiv of F^- (Warburg & Christian, 1941–1942). A large deviation from Warburg's inhibition index was demonstrated by Wang & Himoe (1974) by a careful kinetic analysis of F^- inhibition of rabbit muscle enolase. A better correlation of the inhibition index with $[M^{2+}][P_i][F^-]$ was observed.

The kinetic investigation by Wang & Himoe (1974) demonstrated a large variation in the strength of F^- inhibition as a function of the activating divalent cation. The Mg^{2+} activated enzyme is most strongly inhibited; the Mn^{2+} activated enzyme is inhibited 40 times more weakly, and the Zn^{2+} activated enzyme shows no inhibition by F^-. The effectiveness of F^- inhibition approximates the effectiveness of these cations in activating enolase (V_{max} effects: $Mg^{2+} > Mn^{2+} > Zn^{2+}$). This correlation suggests an analogy between an optimal active-site structure for catalysis and an optimal site for F^- inhibition modulated by the required cation. A similarity between the active-site structure involved in catalysis and inhibition is therefore implied. Dehydration of D(+)-2-PGA by enolase is believed to proceed in a trans fashion (Cohn et al., 1970), via a carbanion intermediate, formed when the C-2 proton of 2-PGA is abstracted (DiNovo & Boyer, 1971; Shen & Westhead, 1973). Subsequent steps involve sp^2 hybridization of C-2 and loss of a hydroxide ion. The hydroxyl group is transferred from 2-PGA to the inner coordination sphere of the metal ion during dehydration (Nowak et al., 1973). Wang & Himoe (1974) have suggested that F^- acts as an analogue of the hydroxyl group and interacts with the activating cation. The data presented in this investigation confirms this view.

In this investigation, it is shown that F^- and P_i form respective ternary complexes with enolase–Mn. The resultant quaternary complex with enolase, Mn^{2+}, and both F^- and P_i can also be formed via a random addition of ligands. The dissociation constants of these ligands from the enzyme complexes are very similar to their respective inhibition constants as measured with rabbit muscle enolase (Wang & Himoe, 1974). The quaternary complex results in the shielding of the bound cation from the solvent isolating the catalytic site and

† From the Department of Chemistry, Program in Biochemistry and Biophysics, University of Notre Dame, Notre Dame, Indiana 46556. *Received February 24, 1981; revised manuscript received July 15, 1981.* This work was supported in part from National Institutes of Health Research Grants AM17049 and AM00486, Biomedical Science Support Grant RR07033-10 from The General Research Resources, Research Corporation, and a Grant-in-Aid from Miles Laboratories, Elkhart, IN.

‡ Recipient of Research Career Development Award AM00486 of the National Institutes of Health.

[1] Abbreviations used: 2-PGA, 2-phosphoglyceric acid; P-enolpyruvate, phosphoenolpyruvate; P_i, orthophosphate; Tris, tris(hydroxymethyl)-aminomethane; NMR, nuclear magnetic resonance; PRR, water proton longitudinal relaxation rates; A, optical absorbance.

0006-2960/81/0420-6894$01.25/0

yielding inactive enzyme. This process prevents the dehydration of PGA from occurring and results in the inhibition of glycolysis.

Materials and Methods

Enolase was prepared from bakers' yeast as described by Westhead & McLain (1964) except that the final batchwise adsorption and elution from cellulose phosphate was replaced by chromatography on DEAE-cellulose at 4 °C. The resin was equilibrated with buffer containing 1 mM Tris-HCl and 1 mM $MgCl_2$, pH 8.0. The enzyme was adsorbed from the same buffer and eluted with a gradient of 0–0.1 M KCl. The major and most active enolase peak was eluted at about 0.045–0.065 M KCl. Polyacrylamide gel electrophoresis of the purified enzyme yielded a single band responsible for at least 98% of the area under a densitometer scan. The purified enzyme had a specific activity of 95–100% of that stated by Westhead & McLain (1964). Trisodium D(+)-2-PGA was obtained from Sigma. The reagents KCl, KF, KOH, KH_2PO_4, $MgCl_2 \cdot 6H_2O$, and $MnCl_2 \cdot 4H_2O$ were all reagent grade. The solutions of P_i were made by titrating KH_2PO_4 with KOH to the desired pH prior to final dilution.

When necessary, solutions (including solutions containing enzyme) were made metal free by passage through a Chelex-100 (Bio-Rad) resin column. This treatment was very important in removing endogenous metal ion contaminants. Distilled deionized water was used routinely for all solutions. The enzyme concentration was determined by using the extinction coefficient $\epsilon_{280} = 0.89$ mL mg^{-1} cm^{-1} (Warburg & Christian, 1941–1942) and the molecular weight 88 000 per dimer (Mann et al., 1970). The enzyme was assayed as described by Westhead & McLain (1964) except that D(+)-2-PGA was used (instead of the racemic mixture) at one-half the stated concentration. The formation of P-enolpyruvate was monitored by using a Gilford 240 spectrophotometer at 240 nm at 30 °C.

UV difference spectra were obtained with a Gilford 240 spectrophotometer with a Model 2530 wavelength scanner attachment. Difference spectra were measured from 240 to 320 nm. Routinely, 1-mL sample solution containing 25 μM enolase (50 μM sites), 200 μM $MnCl_2$, and 50 mM Tris-HCl, pH 7.5, in the presence or absence of 0.5 M KCl were titrated with microliter quantities of ligand solutions. The ionic strength made no difference in the results. Reference solutions were titrated with equivalent volumes of water. Corrections were made in ΔA for dilution of the enzyme from the original 50 μM sites.

Dissociation constants were obtained by fitting the data to the expression

$$\Delta A/\Delta A_{max} = \{K_d + [S]_t + [L]_t - [K_d^2 + [S]_t^2 + [L]_t^2 + 2K_d([S]_t + [L]_t) - 2[S]_t[L]_t]^{1/2}\}/2[S]_t \quad (1)$$

where ΔA is the corrected change in absorbance which is induced by ligand binding at total ligand concentration $[L]_t$ and at total enzyme sites concentration $[S]_t$. The value ΔA_{max} is the change in absorbance obtained by extrapolation to infinite ligand concentration. Note that only total concentrations are used in eq 1, although it yields exact solutions. This is necessary since the relatively large concentrations of enzyme used dictate that free ligand concentratons be significantly smaller than total ligand concentrations except in the case of weak binding. Also, this expression becomes quite insensitive to $[S]_t$ when $K_d \gg [S]_t$.

PRR Measurements. Solvent water proton longitudinal relaxation rates ($1/T_1$) were measured with a Seimco pulsed NMR spectrometer operating at 24.3 MHz using the Carr–Purcell 180°–τ–90° pulse sequence (Carr & Purcell, 1954). The paramagnetic effect on the relaxation rate ($1/T_{1p}$) is the difference in relaxation rates observed for a solution which contains the paramagnetic ion ($1/T_{1,obsd}$) and the relaxation rate of the identical solution in the absence of the paramagnetic species ($1/T_{1,0}$). The observed enhancement parameter (ϵ^*) is the ratio of $1/T_{1p}$ in the presence of the enzyme $(1/T_{1p})^*$ to $1/T_{1p}$ in the absence of the enzyme (Eisenger et al., 1962). The observed enhancement for enzyme and Mn^{2+} in the absence of added ligands will depend on the fraction of Mn^{2+} which is bound to the enzyme and the enhancement for the bound Mn^{2+}, ϵ_b.

For enolase-bound Mn^{2+}, ϵ_b is 13–15 (Cohn, 1963; Nowak et al., 1973). In the presence of ligand, a third enhancement term, ϵ_t, must be considered

$$\epsilon^* = \frac{[Mn^{2+}]_{free}}{[Mn^{2+}]_t}(\epsilon_a) + \frac{[E\text{–}Mn]}{[Mn^{2+}]_t}(\epsilon_b) + \frac{[E\text{–}Mn\text{–}L]}{[Mn^{2+}]_t}(\epsilon_t) \quad (2)$$

An additional ligand requires further consideration. In general, there is an enhancement term (ϵ_b, ϵ_t, ϵ_q, . . .) for each complex of Mn^{2+}, and each contributes to ϵ^* as determined by the relative population of the respective complex with respect to total $[Mn^{2+}]$.

For an investigation of ligand binding by a PRR titration, a sample of enzyme containing Mn^{2+} is titrated with a solution which contains an identical concentration of enzyme and Mn^{2+} and also includes the ligand. In this way, the concentration of the ligand is varied without changing the concentration of the enzyme or Mn^{2+}. The $1/T_1$ of water is measured, and ϵ^* is plotted as a function of ligand concentration. The dissociation constants were obtained by using a computer fitting routine which varies K_d until a minimum is obtained in the standard deviation of ϵ_t calculated at each concentration (Reed et al., 1970). This routine takes into account all possible equilibria including E–L and Mn–L complexes.

For investigation of the effect of temperature on $1/T_{1p}$ of each complex, sufficient enzyme and ligand were added to bind and saturate nearly all the Mn^{2+} so that $1/T_1$ primarily reflects a single species. The values of $1/T_1$ for the diamagnetic controls were subtracted from each observed value to yield $1/T_{1p}$ for each complex at each temperature. Temperature was varied by passing cooled nitrogen over a thermostated heating filament before it arrived at the sample zone. The temperature at the sample within the probe was measured directly by means of a thermocouple.

Results

Formation of the Ternary Complexes. The interaction of F^- with the enolase–Mn complex was investigated by UV difference and by PRR techniques. The addition of F^- induces a UV difference spectrum of the protein–Mn^{2+} complex with a positive maximum at 264 nm (Figure 1). The amplitude of the absorbance difference at this wavelength is dependent on $[F^-]$ and is calculated to be 1220 ± 200 M^{-1} cm^{-1} at saturating concentrations of F^-. When the results of the F^- titration (Figure 2A) are fit to eq 1, a dissociation constant of 0.6 ± 0.2 M is obtained. In these studies, the enzyme is essentially saturated with an excess of metal ion; $[Mn^{2+}]_t/[E]_t = 8.0$.

PRR titrations were also used to investigate the interaction of F^- to the enzyme. The enolase–Mn complex exhibits a binary enhancement of 13–15 (Cohn, 1963; Nowak et al., 1973). Titration of F^- into the E–Mn complex decreases the enhancement value (Figure 3) to yield a ternary enhancement (ϵ_t) of 7.0 ± 0.3 when either 0.7 or 3.0 equiv of Mn^{2+} are

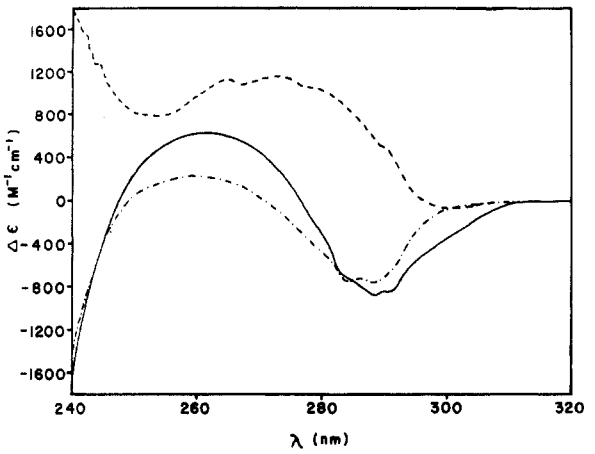

FIGURE 1: Normalized UV difference spectra of enolase–Mn complexes which contain F^- and P_i. Both sample and reference cells contained 25 μM enolase (50 μM sites), 200 μM $MnCl_2 \cdot 4H_2O$, 0.5 M KCl, and 50 mM Tris-HCl, pH 7.5. In addition, the sample cells contained 2 M KF (---), 14 mM P_i (–·–), and 0.1 M KF plus 0.45 mM P_i (—). The difference spectra measured in the absence of KCl were essentially identical. The differences in absorption which were measured were corrected to a 1 M concentration of enzyme.

present per mol of enzyme. This change in enhancement is specific for F^- and is not an ionic strength effect. High concentrations of KCl fail to perturb the enhancement of enolase–Mn or the spectrum of enolase–Mn. An optimal fit to the data in Figure 3 is obtained when K_d is assumed to be 0.6 ± 0.1 M for the formation of the ternary E–M–F complex. These dissociation constants are in agreement with the very weak inhibition of Mn^{2+}-activated enolase by F^- in the absence of P_i with the rabbit muscle enzyme (Cimasoni, 1972; Wang & Himoe, 1974). The K_d value obtained by UV difference and PRR titrations are in excellent agreement.

The interaction of P_i with the E–Mn complex was also investigated by UV difference spectroscopy and by PRR techniques. The normalized UV difference spectrum (E–Mn–P_i vs. E–Mn) is also shown in Figure 1. A negative maximum is shown at 295 nm. At saturating concentrations of P_i, the difference amplitude at this wavelength is calculated to be -630 ± 100 M^{-1} cm^{-1}. A titration of the UV spectral changes by P_i results in a hyperbolic response, and the best fit to eq 1 for this data gives $K_d = 0.3 \pm 0.1$ mM (Figure 2C). As in the F^- studies, an excess of Mn^{2+} ($[Mn^{2+}]_t/[E]_t = 8.0$) is employed.

The effect of P_i on the PRR of the E–Mn complex was also studied. The addition of P_i has a significant effect on the enhancement value, and the ϵ_t for the E–Mn–P_i complex is about 10 (Figure 4). The apparent K_d for P_i is dependent on the ratio of Mn^{2+} to enzyme. When $[Mn^{2+}]/[E]_t = 0.64$, K_d is 1.2 ± 0.2 mM; when $[Mn^{2+}]/[E]_t = 2.5$, K_d is decreased to 0.6 ± 0.1 mM. Apparently higher Mn^{2+} to enzyme ratios result in tighter P_i binding. This observation is consistent with the UV difference study where the binding of P_i resulted in a K_d of 0.3 mM at a Mn^{2+}/E ratio of 8. In kinetic studies where the enzyme concentrations are much lower and the ratio of free Mn^{2+} to enzyme is high, the K_i of P_i with Mn^{2+}-activated rabbit muscle enolase was about 1 mM (Wang & Himoe, 1974).

Formation of the Quaternary Complex. The formation of the quaternary complex of enolase–Mn–F–P_i was studied by UV difference and by PRR techniques. UV difference spectroscopic and PRR titrations reveal that the presence of either one of the ligands, F^- or P_i, greatly increased the affinity of the second ligand for the enzyme–Mn ternary complex. These titrations result in the formation of a tightly bound

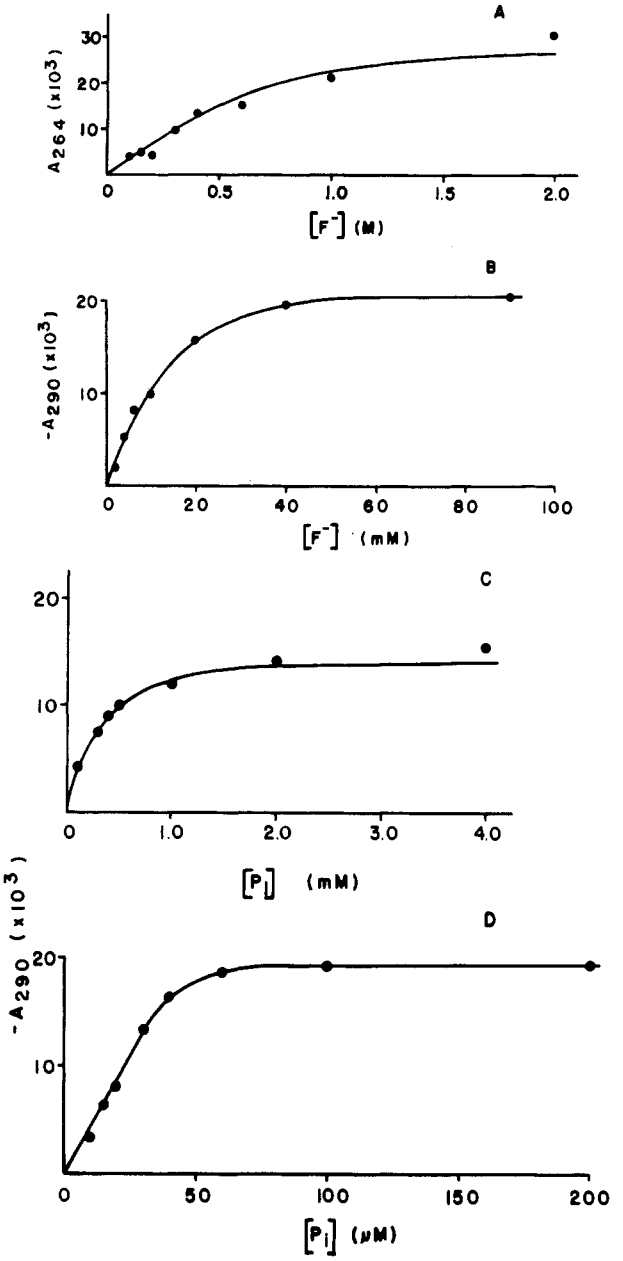

FIGURE 2: UV difference spectra titrations of enolase containing Mn^{2+} with F^- and with P_i. The conditions of each experiment were as described under Materials and Methods except as otherwise mentioned. In (A), an increase in absorbance at 264 nm is monitored as a function of F^- concentration. The curve drawn is a theoretical curve with K_d = 0.6 M. In (B), the solution being titrated also contained 50 μM P_i. A decrease in absorbance at 290 nm is monitored as a function of F^- concentration. The theoretical curve is drawn assuming K_d = 10 mM. In (C), a decrease in absorbance at 290 nm is monitored as a function of P_i. The theoretical curve is drawn assuming K_d = 0.3 mM. In (D), the solution being titrated contained 100 mM KF, and a decrease in absorbance at 290 nm is monitored. The curve is generated assuming K_d = 0.5 μM.

E–Mn–P_i–F quaternary complex. As little as 0.1 mM P_i decreases the apparent K_d of F^- by about 2 orders of magnitude. Figure 5 shows the results of a PRR titration of F^- into the enolase–Mn^{2+} complex in the presence of 1 mM P_i. The final enhancement values observed from these titrations are between 0.4 and 0.8. This low enhancement value suggests that there is no freely accessible solvent water interacting with the Mn^{2+} in the quaternary E–Mn–F–P_i complex. When the $[Mn^{2+}]_t/[E]_t$ ratio is less than unity, the K_d for F^- from the quaternary complex yields a value of 2.4 ± 0.4 mM and ϵ = 0.7–0.8. When such a titration was performed at a $[Mn^{2+}]_t/[E]_t$ of 3.0, the titration data could not be fit by a

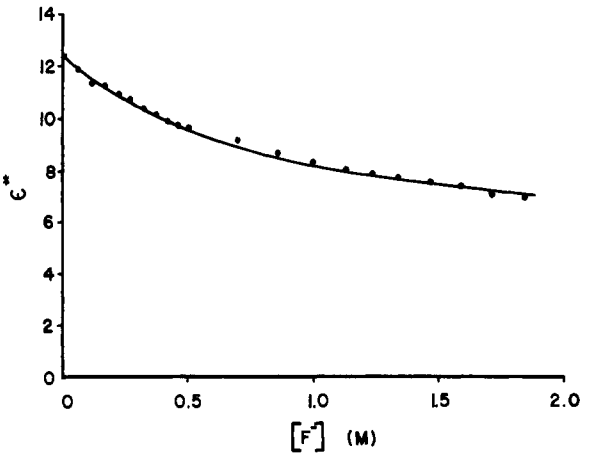

FIGURE 3: PRR enhancement values of enolase–Mn as a function of [F⁻]. A solution containing 57 μM enolase (114 μM sites), 40 μM $MnCl_2 \cdot 4H_2O$, 50 mM KCl, and 50 mM Tris-HCl, pH 7.5, in a 50 μL volume was titrated with an identical solution except that it also contained 3 M KF. The last four points were obtained by titrating with 13.2 M KF. The data were fit by using the following parameters: $\epsilon_b = 14$; $\epsilon_t = 7.01$; $K_3 = 0.6$ M. The fit was insensitive to K_s values >0.1 mM.

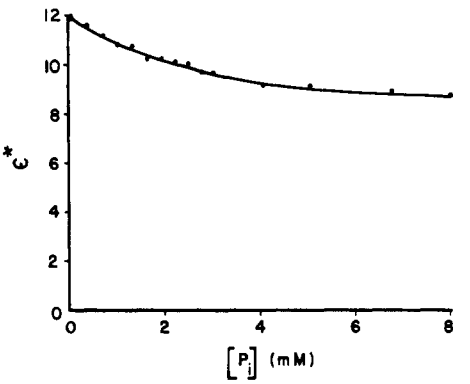

FIGURE 4: PRR enhancement values of enolase–Mn as a function of P_i concentration. A solution containing 79.5 μM enolase (159 μM sites), 200 μM $MnCl_2 \cdot 4H_2O$, 50 mM KCl, and 50 mM Tris-HCl, pH 7.5, in a final volume of 50 μL was titrated with an identical solution except that it also contained 20 mM potassium phosphate, pH 7.5. The last two points were obtained by titrating with 1 M P_i, pH 7.5. The data were fit by using the following parameters: $\epsilon_b = 13.6$; $\epsilon_t = 10.0$; $K_3 = 0.6$ mM. The fit was insensitive to K_s values >0.1 mM.

Scheme I

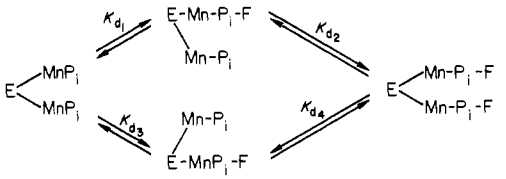

curve generated assuming a single K_d (Figure 6). A fit to the data could be obtained by assuming two equivalent F⁻ sites per enzyme dimer where the occupancy of one site by F⁻ reduced the K_d for F⁻ at the second site. This fit is given in Scheme I. In this scheme $K_{d_1} = K_{d_3} > K_{d_2} = K_{d_4}$. A "best fit" to the data is obtained by using K_{d_1} (and K_{d_3}) = 7.2 mM and K_{d_2} (and K_{d_4}) = 1.0 mM (Figure 6). The values of K_d for F⁻ binding to the E–Mn_2 complex are constant at $[P_i]_t$ > 0.1 mM but become larger at lower levels of P_i. To our knowledge, this is the first evidence for thermodynamically nonequivalent ligand binding to enolase.

It was difficult to obtain a good UV difference spectrum showing the effect of F⁻ addition when the concentration of P_i was above 50 μM. However, at this concentration of P_i,

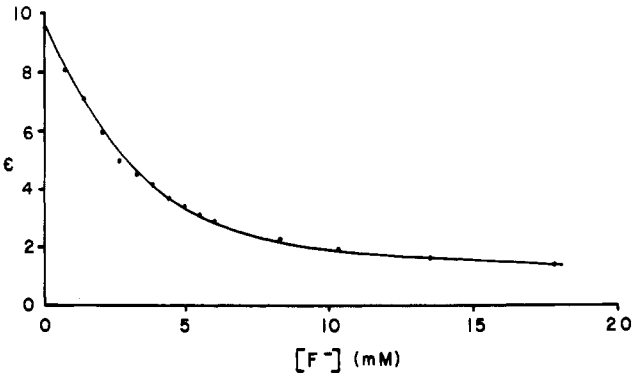

FIGURE 5: PRR enhancement values of enolase–MnP as a function of F⁻ concentration. A solution containing 62.5 μM enolase (125 μM sites), 50 μM $MnCl_2$, 1.8 mM P_i, 50 mM KCl, and 50 mM Tris-HCl, pH 7.5, in a volume of 50 μL was titrated with an identical solution except that it also contained 36 mM KF. The last point was obtained by titrating a sample of 0.36 M KF and correcting the relaxation rate for dilution. The data were fit by using the following parameters: $\epsilon_b = 13.6$; $\epsilon_t = 0.63$; $K_3 = 2.4$ mM. The fit was insensitive to values of K_s >1.0 mM.

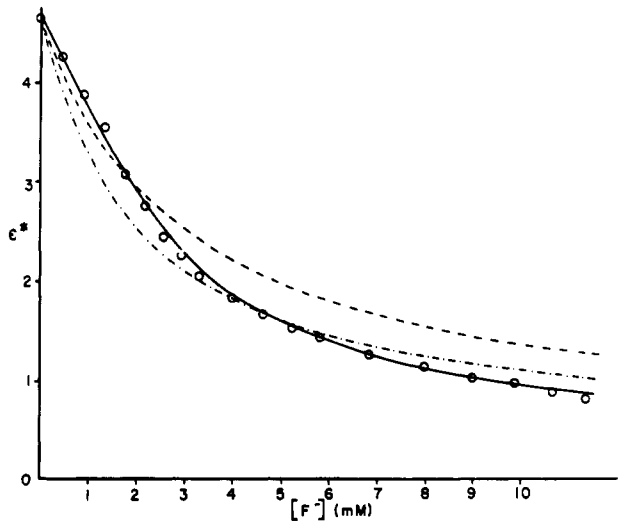

FIGURE 6: PRR enhancement values of enolase–Mn–P_i as a function of [F⁻]. A solution containing 66 μM enolase (132 μM sites), 200 μM $MnCl_2 \cdot 3H_2O$, 1 mM P_i, 50 mM KCl, and 50 mM Tris-HCl, pH 7.5, was titrated with an identical solution except that it also contained 24 mM KF. The sample volume was initially 50 μL, and a total of 45 μL of titrant was added. The broken lines represent theoretical curves representing dissociation constants of F⁻ from the ternary complex of 3 mM (---) and 2 mM (-·-). The solid line represents a theoretical curve derived from Scheme I using $K_{d_1} = K_{d_3} = 7.2$ mM and $K_{d_2} = K_{d_4} = 1.0$ mM.

the difference absorbance values found for a titration with F⁻ gave a best fit to eq 1 of K_d = 10 mM (Figure 2B). At this concentration of P_i, the system is not fully saturated. Thus, the effect of P_i on the K_d of F⁻ is not fully manifested.

In agreement with thermodynamic expectations, the apparent K_d of P_i also decreases dramatically in the presence of F⁻. The results of one such PRR titration are shown in Figure 7. In this titration, the final enhancement value is about 0.6 when P_i is titrated into a solution of the enzyme and Mn^{2+} containing 200 mM KF. In the case of P_i binding to form the quaternary complex, the dissociation constant is effected by the ratio of Mn^{2+} to enzyme. Thus at $[Mn^{2+}]/[E]_t = 0.65$, the K_d value for P_i binding is 19 ± 2 μM, whereas when the ratio is increased to 2.8 Mn^{2+} per enzyme, the K_d is as low as 1 μM. The titration curves could be fit by a single value for K_d for P_i from the E–Mn–F–P_i complex, however. Figure 7 (inset) shows the apparent K_d for P_i binding to form the quaternary complex as a function of F⁻ concentration.

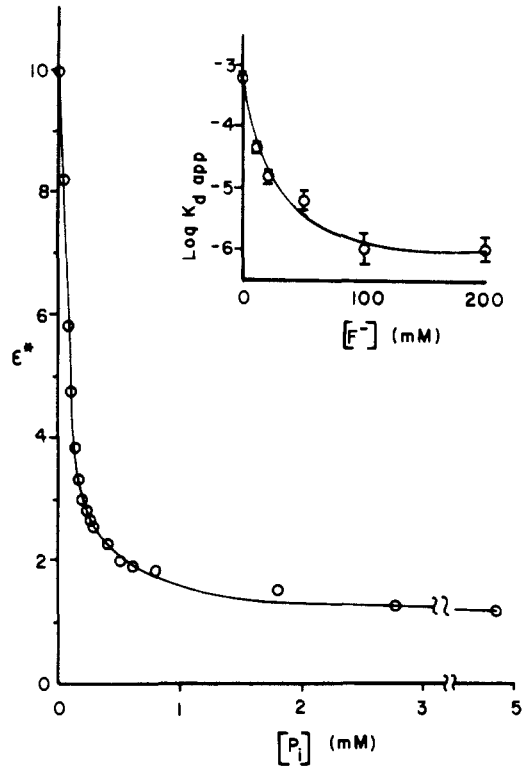

FIGURE 7: PRR enhancement values of enolase–Mn–F as a function of P_i concentration. A solution containing 70 μM enolase (140 μM sites), 200 mM $MnCl_2 \cdot 4H_2O$, 200 mM KF, 50 mM KCl, and 50 mM Tris-HCl, pH 7.5, in a volume of 50 μL was titrated with an identical solution except that it also contained 0.5 mM P_i, pH 7.5. The last two points were obtained by titrating with 1 M P_i, pH 7.5. In the inset, the log of the dissociation constant for P_i binding to enolase–Mn as a function of the total concentration of F^- present is shown. Each sample contained 70 μM enolase (140 μM sites), 200 M $MnCl_2 \cdot 4H_2O$, 50 mM KCl, 50 mM Tris-HCl, pH 7.5, and 0–200 mM KF as indicated. The titrant was an identical solution except that it also contained 0.5 mM P_i, pH 7.5. For the experiment with no KF, the titrant contained 20 mM P_i, pH 7.5. The titrations and the data analysis were performed as detailed under Materials and Methods.

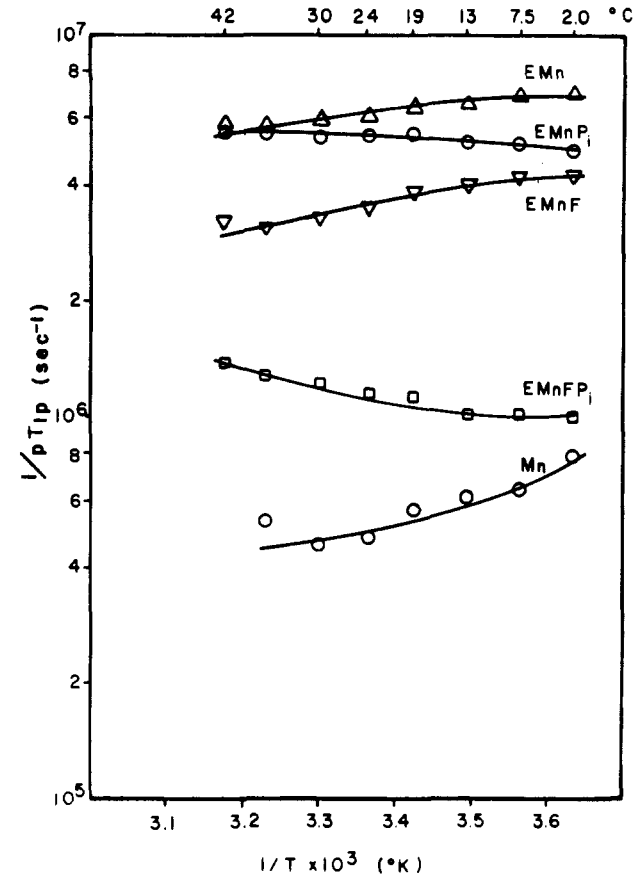

FIGURE 8: Values of $1/pT_{1p}$ of solvent water protons in the presence of various Mn^{2+} complexes as a function of reciprocal temperature (K^{-1}). Each sample excluding the Mn^{2+} $(H_2O)_6$ control contained 108 μM enolase (216 μM sites). Each sample also contained 50 mM KCl and 50 mM Tris-HCl, pH 7.5. The solutions contained 20 mM P_i, 2 M KF, and 0.2 M KF plus 1 mM P_i for the E–Mn–P_i, E–Mn–F, and E–Mn–F–P_i complexes, respectively. Each experimental value is an average of two measurements at each temperature. The data was normalized by the factor p (ratio of $[Mn^{2+}]$ to $[H_2O]$). The duplicate experiments were performed at 12.05 and at 24.1 μM Mn^{2+}, and the concentration of water (55.5 M) was used rather than the concentration of protons (111 M).

In Figure 2D, the titration of the E–Mn–F complex by P_i using UV difference changes is shown. The P_i was titrated into a solution of enzyme, Mn^{2+}, and F^- with $[Mn^{2+}]_t/[E]_t = 8.0$, and the K_d was found to be 0.5 ± 0.2 μM.

The effect of F^- on the binding of the competitive inhibitor phosphoglycolate to the enolase–Mn complex was also investigated. The dissociation constant of this ligand was measured by analogous PRR titrations in the presence and absence of F^-. The results showed that the K_d of phosphoglycolate actually increased from about 0.3 mM to about 0.6 mM in the presence of 0.1 M F^- with 2.5 equiv of Mn^{2+} per enolase dimer. Thus, the positive cooperativity in binding induced by F^- appears specific for P_i.

In a kinetic experiment (P. J. Maurer and T. Nowak, unpublished results), the use of fluorophosphate (FPO_3^{2-}) in lieu of P_i failed to elicit any substantial cooperative inhibition in the presence of F^- in contrast to the cooperative effect observed with F^- and P_i. These results further demonstrate the specificity of the phosphate anion in the cooperative inhibition with F^-.

Temperature Effects on the PRR Values of Enolase–Mn Complexes. The decrease in enhancement observed for each of the complexes studied relative to the binary enolase–Mn complex could be interpreted by several models. The temperature dependence of the relaxation rates was investigated to attempt to elucidate the mechanisms for these effects. The solutions were prepared such that the distribution of Mn^{2+} was primarily in a single enzyme–Mn–ligand complex. The relaxation rates of diamagnetic controls (identical solutions except for the absence of Mn^{2+}) were subtracted from the observed relaxation rates to obtain $1/T_{1p}$ for each complex as a function of temperature. The $1/T_{1p}$ values were normalized by dividing by p (the ratio of Mn^{2+} to water concentrations), thus yielding $1/pT_{1p}$ for $(Mn \cdot 6H_2O)^{2+}$, enolase–Mn, enolase–Mn–F, enolase–Mn–P_i, and enolase–Mn–F–P_i. The data obtained for each species are plotted as log $1/pT_{1p}$ vs. $1/T$ (K^{-1}) in Figure 8.

It is noted that enolase–Mn has a high enhancement relative to $(Mn \cdot 6H_2O)^{2+}$ at all temperature studied. This indicates that nearly all the Mn^{2+} is enzyme bound. The data for enolase–Mn–F parallel that for enolase–Mn and yield relaxation rates approximately one-half of the latter. The data for EMP are quite different in that the relaxation rates approach those of the enolase–Mn complex with increasing temperature. These data suggest that P_i places an additional energy barrier on the water or proton exchange process which can be overcome by raising the available thermal energy. These results suggest that P_i does not displace any water molecules from the first coordination sphere of the enzyme-bound Mn^{2+}. In the case of E–Mn–F–P_i, the relaxation rates are drastically lower than for E–Mn, indicating that the Mn^{2+}-bound water is highly immobile or inaccessible to the bulk solvent. The

Table I: Dissociation Constants of Ligands from Ternary and Quaternary Complexes

complex	ligand	$[Mn^{2+}]_t/[enolase]_t$	ϵ	ΔA_{max} (M^{-1} cm^{-1})	λ_{max} (nm)	K_d
E-Mn-F[a]	F^-	0.7	7			0.6 M
E-Mn-F[a]	F^-	3.0	7			0.6 M
E-Mn-F[b]	F^-	8.0		+1220	264	0.6 M
E-Mn-P_i[a]	P_i	0.64	10			1.2 mM
E-Mn-P_i[a]	P_i	2.5	10			0.6 mM
E-Mn-P_i[b]	P_i	8.0		−630	295	0.3 mM
E-Mn-F-P_i[a]	F^-	0.64	0.7			2.4 mM
E-Mn-F-P_i[a]	F^-	3.0	0.4			7.2 mM/1.0 mM[c]
E-Mn-F-P_i[b]	F^-	8.0		−824	290	<10 mM
E-Mn-F-P_i[a]	P_i	0.65	0.6			19 μM
E-Mn-F-P_i[a]	P_i	2.8	0.6			1 μM
E-Mn-F-P_i[b]	P_i	8.0		−768	290	0.5 μM

[a] Determined by a PRR titration. [b] Determined by a UV difference titration. [c] Requires two K_d values to fit the data as discussed in the text.

slope of the plot is negative and nearly linear, indicating that the observed relaxation rates of water may be limited by slow chemical exchange in the quaternary complex. The Mn^{2+}-induced relaxation may also be a second sphere effect in the quaternary complex.

Discussion

The reaction catalyzed by enolase plays a key role in anaerobic metabolism whereby 2-PGA which has a small negative free energy of hydrolysis is reversibly converted to P-enolpyruvate which has a large negative free energy of hydrolysis.

The mechanism of fluoride inhibition of enolase was investigated by a study of the ligand binding properties of F^- and of P_i to the enzyme–Mn complex to form the ternary and quaternary complexes.

UV difference spectral studies of ligand binding were performed at a ratio of 8 Mn^{2+} per enolase dimer. Under these conditions, both F^- and P_i induce characteristic UV difference spectra of the E–Mn complex which show spectral changes reflecting simple, saturable, hyperbolic binding curves as a function of ligand concentration (Figure 2). The difference spectra demonstrate specific ligand-induced conformational changes resulting from the formation of the ternary E–Mn–F and E–Mn–P_i complexes. The dissociation constants obtained from a titration of these spectral changes agree very closely with inhibition constants for the same ligands (Wang & Himoe, 1974), indicating that it is the ligand–protein interaction which causes inhibition. Formation of the quaternary complex could also be detected by UV difference techniques by titrating either ternary complex with the remaining ligand. The difference spectrum of the quaternary complex more closely resembles that of the E–Mn–P_i ternary complex than that of the E–Mn–F complex. Titration experiments to form the quaternary complex yield binding curves with dissociation constants up to nearly 3 orders of magnitude lower than those for formation of ternary complexes. Such a high degree of cooperativity in ligand binding explains the contrast between the weak inhibition caused by either F^- or P_i alone and the strong inhibition caused by combinations of F^- and P_i. The spectral changes demonstrate differences in the protein structure for the ternary and quaternary complexes.

The PRR titrations of E–Mn with F^- at either <1 or 2–3 Mn^{2+} per dimer showed no differences in results with $\epsilon_t = 7.0 \pm 0.3$ (Figure 3) and $K_d = 0.6 \pm 0.1$ M. In contrast, the binding of P_i to enolase–Mn became tighter as levels of Mn^{2+} were increased. This effect may be analogous to the decrease in the K_m of 2-PGA upon increasing the Mn^{2+} concentration (Nowak et al., 1973; Wang and Himoe, 1974).

In the formation of the quaternary complex, the binding of both ligands was affected by the levels of Mn^{2+} in the particular experiment, but in different ways. In the measurement of P_i binding, the K_d decreased upon increasing Mn^{2+} concentration, analogous to the formation of the ternary E–Mn–P_i complex. A free energy of cooperativity of binding (Nowak & Lee, 1977) of −2.5 to −3.8 kcal/mol elicited by the presence of F^- is calculated. With F^- binding to E–Mn–P_i, the effect of the Mn^{2+} to enzyme ratio was different. At a stoichiometry of <1 Mn^{2+} per enzyme, a simple binding plot with K_d = 2.4 mM was obtained, and a $\Delta(\Delta G°)$ of binding of −3.3 kcal/mol is calculated. At a Mn^{2+}/enolase ratio >1, the PRR titration data could not be fit by assuming simple ligand binding. The data could be fit, however, by invoking positive cooperativity between two equivalent F^- binding sites. Other models, such as random or sequential binding at two distinct nonequivalent sites, may also fit the data equally well, however. The binding curves generated from these models are usually similar. The data could be fit by using K_d values of 7.2 mM and 1.0 mM for the two F^- binding sites. $\Delta(\Delta G°)$ values of −2.6 and −3.8 kcal/mol were calculated for the cooperative free energy of binding at both sites.

Interestingly, this nonequivalence of F^- binding thermodynamics was not detected by UV difference measurements. This may be a function of lack of sensitivity of the observed effect or may reflect a lack of chromophoric perturbation by the binding of F^- at the "second" (thermodynamically distinct) site. The detection of thermodynamically nonequivalent F^- binding sites in the quaternary complex is the first such evidence for nonequivalent ligand binding to enolase. Nonequivalent binding sites for cations, however, have been observed (Hanlon & Westhead, 1969).

This cooperative binding of ligands is among the largest reported in the literature for reciprocally cooperative multiple ligand binding to a protein with $\Delta(\Delta G°)$ values of −2.5 to −3.8 kcal/mol. The dissociation constants were obtained by assuming one ligand binding per active site to form the complex. A summary of the dissociation constants measured for the formation of the ternary and quaternary complexes is presented in Table I. The detection and quantitative determination of the ternary and quaternary complexes indicate a random addition of ligands to form the potent inhibitory quaternary complex via Scheme II.

Direct metal ion binding studies to enolase and enolase-containing substrate (Hanlon & Westhead, 1969; Faller et al., 1977; Faller & Johnson, 1974) and kinetic studies of metal activation of enolase activity (Nowak et al., 1973; Wang & Himoe, 1974) indicate a reciprocal effect of cation binding and ligand binding to enolase. The effect of the activating

Scheme II

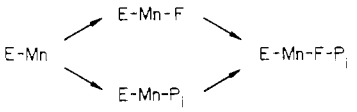

cation upon the strength of F^- inhibition of enolase (Wang & Himoe, 1974) suggests that F^- interacts directly with the bound cation. The similarity in binding constants of F^- to Mn^{2+} (K_d = 0.3 M) and to enolase–Mn (K_d = 0.6 M) also suggests a direct Mn^{2+}–F^- interaction.

The simplest model proposed to explain the PRR data is the displacement of one of the two water molecules coordinated to enolase–Mn (Nowak et al., 1973) by F^-. The P_i can interact with the bound Mn^{2+} in a second sphere complex via hydrogen bonding through a water molecule. This structure is analogous to the interaction of the bound Mn^{2+} with the phosphoryl group of the substrate demonstrated by high-resolution NMR studies of the ternary enzyme–Mn–substrate complex (Nowak et al., 1973). These structures are verified by high-resolution ^{19}F and ^{31}P relaxation rate studies of the ternary and quaternary complexes (Nowak & Maurer, 1981).

The results of a temperature study of PRR effects are shown in Figure 8. The results of a temperature study of $1/pT_{1p}$ of the binary E–Mn and the ternary E–Mn–F complexes show parallel effects. The relaxation rate for the ternary complex is one-half that for the binary complex, suggesting that one of the two bound water molecules has been displaced by F^-. In the ternary complex containing P_i, however, the relaxation rate approaches that for the binary complex at a higher temperature. The data is consistent with the P_i interacting with the bound Mn^{2+} via an intervening water molecule. The hydrogen-bonded complex decreases the exchange rate of the proton of water involved in the complex formation. Increasing the temperature increases the exchange rate of the proton in the hydrogen-bonded complex until fast exchange is obtained. These models are verified by an estimation of the correlation time (τ_c) for the Mn^{2+}–water interactions in the enzyme–Mn complexes. The values for τ_c were estimated by a measure of the T_{1p}/T_{2p} ratio for water–proton interactions at 100 MHz using the method described by Navon (1970). The values for τ_c for the E–Mn, E–Mn–P_i, and E–Mn–F complexes were estimated as $(3.9 \pm 1.2) \times 10^{-9}$ s, $(5.3 \pm 0.8) \times 10^{-9}$ s, and $(6.6 \pm 1.0) \times 10^{-9}$ s, respectively.

No substantial differences in τ_c or $f(\tau_c)$ are obtained, thus justifying our interpretations of the PRR results. The data are consistent with two, two, and one rapidly exchanging water molecules bound to the Mn^{2+} in the respective complexes. Upon formation of the quaternary complex, an additional conformational change and a low quaternary enhancement are observed. This complex has a water molecule displaced by the bound F^-, and the P_i interacts with the Mn^{2+} via an intervening water molecule. The low enhancement (ϵ_q = 0.7) is explained either by slow exchange of the hydrogen-bonded water molecule or by a second sphere relaxation mechanism. The activation energy for relaxation (E_{act} = 1.6 kcal/mol) is consistent with either mechanism. Either mechanism results in a bound Mn^{2+} which is highly hindered from the solvent.

Acknowledgments

We thank Donald Schifferl for his assistance with the pulsed NMR spectrometer.

References

Carr, H. Y., & Purcell, E. M. (1954) *Phys. Rev. 94*, 630–638.
Cimasoni, G. (1972) *Caries Res. 6*, 93–102.
Cohn, M. (1963) *Biochemistry 2*, 623–629.
Cohn, M., Pearson, J. E., O'Connell, E. L., & Rose, I. A. (1970) *J. Am. Chem. Soc. 92*, 4095–4098.
DiNovo, E. C., & Boyer, P. D. (1971) *J. Biol. Chem. 246*, 4586–4593.
Eisenger, J., Shulman, R. G., & Szymanski, B. M. (1962) *J. Chem. Phys. 36*, 1721–1729.
Faller, L. D., & Johnson, A. M. (1974) *Proc. Natl. Acad. Sci. U.S.A. 71*, 1083–1087.
Faller, L. D., Baroudy, B. M., Johnson, A. M., & Ewall, R. X. (1977) *Biochemistry 16*, 3864–3869.
Hanlon, D. P., & Westhead, E. W. (1969) *Biochemistry 8*, 4247–4255.
Mann, K. G., Castellino, F. J., & Hargrave, P. A. (1970) *Biochemistry 9*, 4002–4007.
Navon, G. (1970) *Chem. Phys. Lett. 7*, 390–394.
Nowak, T., & Lee, M. J. (1977) *Biochemistry 16*, 1343–1349.
Nowak, T., & Maurer, P. J. (1981) *Biochemistry* (following paper in this issue).
Nowak, T., Mildvan, A. S., & Kenyon, G. L. (1973) *Biochemistry 12*, 1690–1701.
Reed, G. H., Cohn, M., & O'Sullivan, W. J. (1970) *J. Biol. Chem. 245*, 6547–6552.
Shen, T. Y. S., & Westhead, E. W. (1973) *Biochemistry 12*, 3333–3337.
Wang, T., & Himoe, A. (1974) *J. Biol. Chem. 249*, 3895–3902.
Warburg, O., & Christian, W. (1941–1942) *Biochem. Z. 310*, 384–421.
Westhead, E. W., & McLain, G. (1964) *J. Biol. Chem. 239*, 24640–2468.
Wold, F., & Ballou, C. E. (1957) *J. Biol. Chem. 227*, 301–312.